



Photoablation with sub-10 fs laser pulses

M. Lenzner^{a,*}, F. Krausz^a, J. Krüger^b, W. Kautek^b

^a *Abteilung Quantenelektronik und Lasertechnik, Technische Universität Wien, Gusshausstrasse 27-29, A-1040 Wien, Austria*

^b *Laboratorium für Dünnschichttechnologien, Bundesanstalt für Materialforschung und-prüfung, Unter den Eichen 87, D-12205 Berlin, Germany*

Received 1 June 1999; accepted 21 July 1999

Abstract

Ablation experiments in several glasses with single and multishot irradiation by laser pulses in the 10-fs pulse duration domain are presented; physical and technological implications are discussed. We demonstrate that these short pulses offer the potential for lateral and vertical machining precision of the order of 100 nm. © 2000 Elsevier Science B.V. All rights reserved.

PACS: 78.47. + p; 42.65.Re

Keywords: Ablation; Laser pulses; Femtosecond pulses

1. Introduction

Material processing with femtosecond pulses is especially interesting in transparent media because it relies on the generation of free electrons by nonlinear processes before significant energy absorption in the lattice occurs. The nonlinear processes that may give rise to dielectric breakdown are avalanche and multiphoton ionization (MPI). Laser induced breakdown has been investigated in a wide range of transparent media including polymers [1–3], calcium fluoride [4,5], magnesium fluoride [6], fused silica [3,5,7–9], sapphire [6,10], glasses [3,6] and biotissue of collagen basis [11–13]. For longer pulses (pulse duration ≥ 10 ps), it is known that plasma generated

by the leading edge of the pulses increases the reflectivity of the irradiated material and prevents part of the energy of the pulse from penetrating. This phenomenon is absent with femtosecond pulses allowing a more efficient energy coupling to the target. On the other hand, for longer pulses, substantial heat diffusion occurs during the laser pulse, resulting in a significant heat affected zone leading to melting and resolidification. By contrast, ultrafast energy deposition with subpicosecond laser pulses vaporizes and ablates the illuminated volume before thermal relaxation sets in. Because most of the deposited energy is removed in the ablated material the ablated area neighborhood remains unaffected, improving the spatial resolution of the processed structures.

This improvement in machining quality by using subpicosecond pulses instead of multi-picosecond to nanosecond duration pulses has been reported previously [9,10]. The purpose of the present study was to investigate machining precision and morphology of

* Corresponding author. Tel.: +43-1-58801-35930; fax: +43-1-58801-35997.

E-mail address: lenzner@iaee.tuwien.ac.at (M. Lenzner).

dielectrics when the pulse duration is further decreased down to the 10-fs regime.

2. Experimental

The femtosecond-laser system used in these experiments is described in Ref. [14]. It is able to generate 5-fs pulses with a peak power of 0.1 TW at a carrier wavelength of 780 nm in a diffraction limited beam at a repetition rate of 1 kHz. The key element in this system is a hollow fiber filled with Argon gas to broaden the spectrum of the amplified 25-fs pulses from a multipass Ti:sapphire amplifier [15]. Bandwidth-limited pulses with durations between 5 and 25 fs can be generated by varying the argon gas pressure in the hollow fiber. Pulse durations of $\tau > 25$ fs are realized by evacuating the fiber and temporally stretching the pulses in blocks of glass in front of the fiber. The capillary acts as an efficient spatial filter for all pulse durations and results in a nearly smooth Gaussian intensity profile on the target. The 5-fs pulses have been attenuated by placing a pair of 2-in. pellicles in the beam with a variable angle of incidence. This setup allows a variable, nearly dispersion-free attenuation up to a factor of 10. The beam is then focussed down to a spot of ≈ 30 μm diameter with a silver mirror. However, the spot size was subject to slight variation for different pulse durations, probably due to some slight nonlinear spatial beam distortion in front of the fiber. Therefore, we imaged the focus onto a CCD camera in order to be able to calculate precisely the fluence for every pulse duration.

For 5-fs pulses visible plasma formation at normal air pressure was observed for several 10 μJ in the case of our focussing geometry. Interaction of this plasma with the propagating pulse can lead to substantial temporal broadening. Therefore, we checked the fringe resolved autocorrelation of these pulses after the focus and verified that no significant broadening took place for the energy range relevant for our experiments. In addition we repeated one of the breakdown experiments at 5 fs pulse duration in vacuum and found no difference in the observed threshold compared to that measured in an atmospheric environment.

Two dielectric materials with bandgaps of $E_g \approx 4$ eV, barium aluminum borosilicate glass (BBS),

Corning 7059, 1-mm thick, and $E_g \approx 9$ eV, fused silica (FS), Corning 7940, 0.2 mm thick were treated. The surface roughness of the glass samples were ≈ 13 nm for BBS and ≈ 10 nm for FS, respectively, and the glass transformation temperatures differ extremely (593°C for BBS, 1050°C for FS).

A major question in laser-induced damage experiments is that of the evaluation of the achieved structures. One of the more accurate, post-experimental methods is the spatial measurement of the generated ablation craters for an energy range as wide as possible and the extrapolation of characteristic quantities such as depth, diameter, or volume to zero [16]. Here, a necessary condition is that the aspect ratio of the holes, i.e., depth divided by diameter, is not too large (≤ 1) so that all the ablated material can leave the crater. Similar procedures for the damaged area have been employed to extrapolate the damage thresholds of transparent solids [17] and to measure the melting threshold in laser induced solid–liquid transitions [18]. As it will be shown here, we successfully used this method to evaluate optical damage thresholds for dielectrics down to the shortest pulses of 5-fs duration.

3. Results and discussion

3.1. Lateral and vertical precision

First we consider the lateral precision of ablation which is an important parameter for micromachining applications. It may even be extended into the sub-micron range, as demonstrated, e.g., for silver [9]. In order to relate the lateral dimensions of the generated structures to the laser spot size, a ‘‘lateral extension parameter’’ q can be defined. It is the ratio between the observed cross-section area of the ablated crater and the illuminated area of a Gaussian beam. The latter is bounded by the fluence decrease to $1/e^2$ of the peak fluence F_0 . If we consider ablation to be limited to the area where the local fluence $F(x, y)$ exceeds the threshold fluence F_{th} , q is given by:

$$q = \frac{1}{2} \ln \left(\frac{F_0}{F_{th}} \right) \quad (1)$$

Fig. 1 shows a semi-logarithmic plot of $q(F_0)$ obtained experimentally for FS at $\tau = 5, 12, 120,$ and 220 fs. The solid lines depict the predictions of Eq.

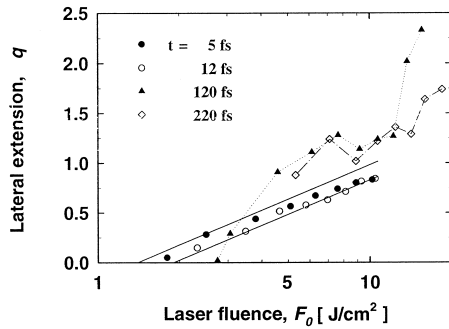


Fig. 1. Lateral extension parameter q vs. laser fluence F_0 for the ablation of fused silica (FS) at air. $\lambda = 780$ nm, $N = 50$, (●) $\tau = 5$ fs, (○) $\tau = 12$ fs, (▲) $\tau = 120$ fs, (◇) $\tau = 220$ fs. The straight lines are calculated from Eq. (1) with the values $F_{th}(\tau = 5 \text{ fs}) = 1.4 \text{ J cm}^{-2}$ and $F_{th}(\tau = 12 \text{ fs}) = 1.9 \text{ J cm}^{-2}$, taken from Ref. [19].

(1) calculated by using the values of $F_{th}(\tau)$ obtained previously from ablation volume measurements [19] for $\tau = 5$ and 12 fs, respectively. For pulse durations $\tau > 100$ fs the observed $q(F_0)$ -dependence strongly deviates from the theoretically predicted straight line. Furthermore, q increasingly exceeds unity, indicating that ablation is not restricted to the area defined by $F(x, y) > F_{th}$. In contrast, in the 10-fs regime the measured $q(F_0)$ shows good agreement with the predictions of Eq. (1) and excellent accordance with F_0/F_{th} in the entire range investigated above threshold. These results and similar results obtained for BBS conclusively demonstrate that laser pulses in the 10-fs regime offer a significantly improved lateral ablation precision in dielectrics as compared to their subpicosecond counterparts.

Shortening the machining pulse duration leads to an increased ablation accuracy also vertically. This has been inferred from a series of measurements of the ablation depth as a function of the number of laser shots [19]. These measurements not only yield the ablation rate, i.e., the depth d of crater produced by one pulse averaged over many shots, but also allow the determination of shot-to-shot deviation of the ablation depth from its mean value. The values of the ablation depth shown in Fig. 2 represent 99% confidence intervals. The tendency of increased vertical ablation precision with decreasing pulse duration is evident for both investigated materials. This trend is expected to become even more pronounced

if data obtained at constant F_0/F_{th} rather than constant F_0 are compared. Our results indicate that laser pulses in the 10-fs regime offer a vertical ablation precision of the order of 10 nm in dielectrics.

These findings strongly suggest the onset of a nonlinear absorption process in the BBS where the absorption gets stronger (i.e., lower penetration depth) for higher intensities. It has been demonstrated [20] in connection with ablation in the nanosecond to picosecond time domain that, considering avalanche ionization as the dominant carrier generation process, the seed electrons for this multiplication have to be supplied by thermal excitation from impurity states into the conduction band. Firstly, this is an inherently statistical process. Secondly, assuming a carrier density of 10^{10} cm^{-3} (e.g., from thermally ionized shallow traps) one can estimate a probability < 1 for the presence of a single seed electron in an interaction volume equal to an ablated volume of 10^{-11} cm^3 (which is a typical value for our geometries). This explains the stochastic character of ablation with longer pulses. Multiphoton ionization comes into play for shorter pulses with higher peak intensities, supplying a larger number of seed electrons for the subsequent avalanche ionization process [19].

3.2. Morphology

Typical scanning electron micrographs (SEM) of four representative ablation craters obtained with

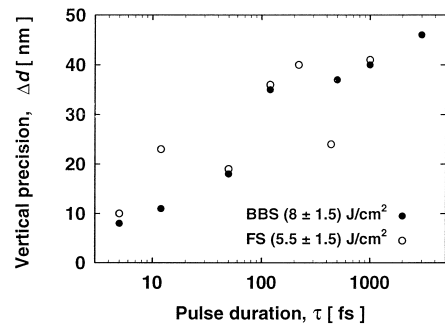


Fig. 2. Absolute vertical precision of ablation for different pulse durations, derived from the 99% confidence interval of the slope of ablation curves (ablation depth vs. number of pulses), for fused silica and BBS.

pulse of durations between 5 fs and 3 ps are shown in Fig. 3. All craters were machined with 80 pulses. The results show increased vertical and lateral precision for shorter pulses. Both the surface and the edge quality of the machined structures are improved by shorter pulses. The 5-fs ablation morphology (Fig. 3d) is far better controlled by the laser beam profile than for $\tau > 100$ fs (Fig. 3a and b). Differences are visible even for the 20-fs pulses (Fig. 3c). In the 3-ps case, the crater edge is heavily broken. The bottom of the 5-fs crater exhibits the same flat surface structure as the original sample surface. This latter result is supported by investigations performed with an atomic force microscope (AFM, see Section 3.3).

3.3. Incubation

Incubation phenomena have been investigated also and found to be more pronounced for fluences close to the ablation threshold and for longer pulse durations. Incubation relates to the phenomenon that a minimum number of pulses have to be applied to the material before macroscopic material removal occurs. It was estimated that incubation in fused silica is absent at $\tau = 5$ fs for $F_0/F_{th} \geq 4$. At this fluence a single 5-fs pulse already led to the ablation of a thin layer without the need of preceding incubating pulses. The generated crater exhibits the same lateral dimensions as achieved with 60 identical 5-fs pulses.

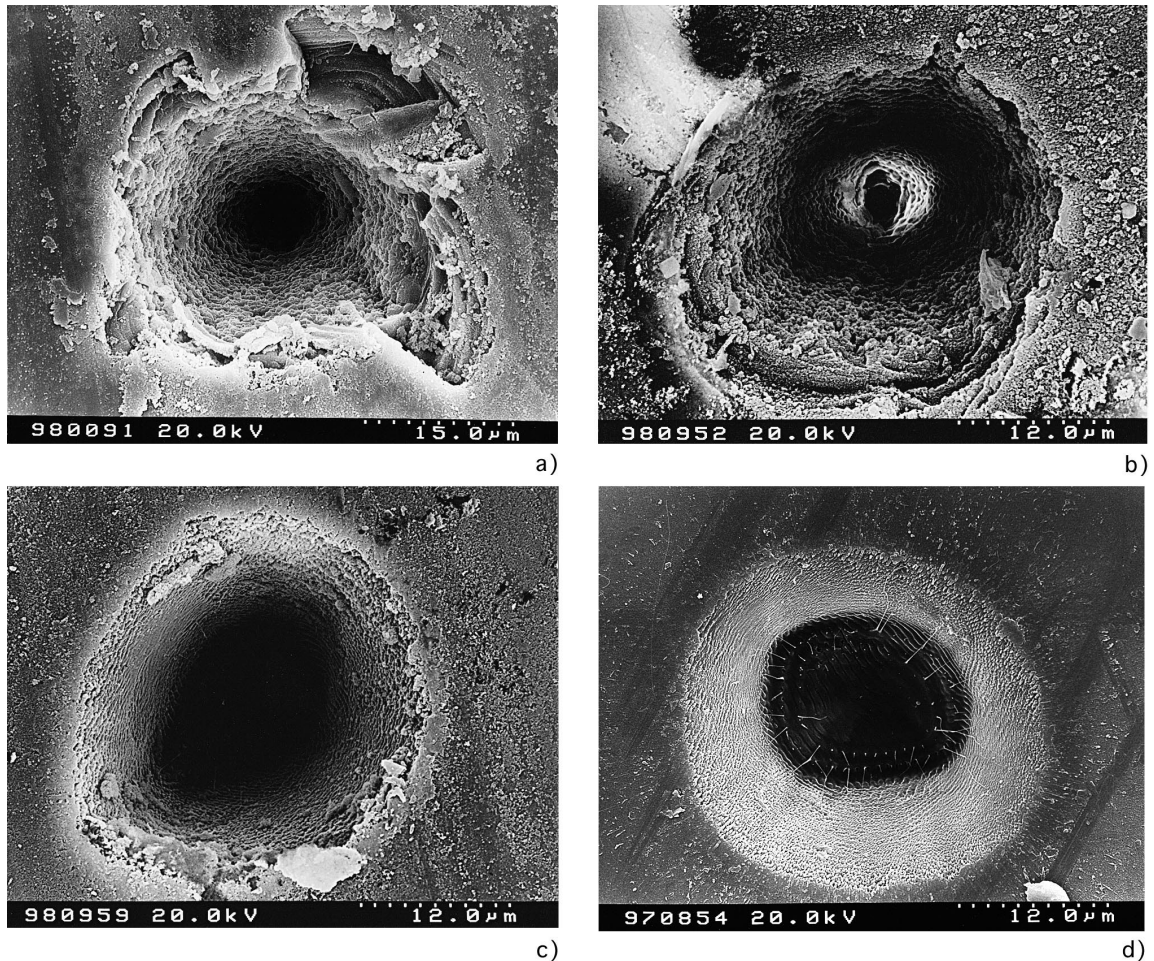


Fig. 3. SEM micrographs of pulse laser ablated fused silica at air. $\lambda = 780$ nm, 80 shots. (a) $\tau = 3$ ps, $F_0 = 19.9$ J cm $^{-2}$, (b) $\tau = 220$ fs, $F_0 = 10.7$ J cm $^{-2}$, (c) $\tau = 20$ fs, $F_0 = 11.1$ J cm $^{-2}$, (d) $\tau = 5$ fs, $F_0 = 6.9$ J cm $^{-2}$.

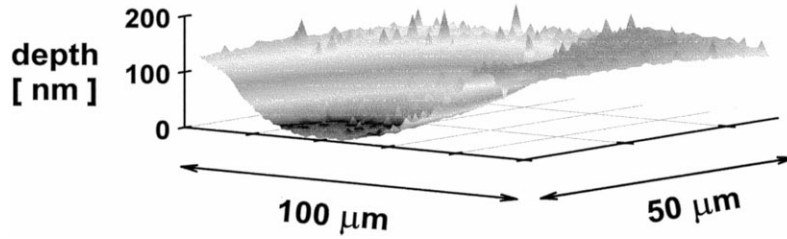


Fig. 4. AFM picture of a laser-generated hole in fused silica, obtained with a single pulse of $\lambda_{\text{center}} = 780 \text{ nm}$, $\tau = 5 \text{ fs}$, $F = 9.5 \text{ J cm}^{-2}$.

Due to the low depth of the crater generated with a single laser pulse ($< 1 \mu\text{m}$) an AFM (Digital Instruments, Dimension 3000 SPM) operated in tapping mode was used to determine the extensions of the structure. A typical picture of an ablation crater is shown in Fig. 4. This hole was produced at a laser fluence of $F = 9.5 \text{ J cm}^{-2}$, which will be shown below to be about twice the damage threshold fluence of this material for single pulses. The 5-fs crater shows a very smooth surface compared to cavities generated with single pulses of several-hundred-femtosecond and picosecond duration.

The ablated volumes for a range of laser fluences above the damage threshold are represented by the dots shown in Fig. 5. Calculating a linear regression (solid line in Fig. 5) and extrapolating this line to an ablated volume of zero yields a threshold fluence of

$F_{\text{th}} = 4.9 \text{ J cm}^{-2}$ for fused silica irradiated with 780 nm pulses of 5 fs duration.

We compared results from earlier experiments with similar experimental parameters, but with each site irradiated with 50 consecutive pulses [19], which are shown as open circles in Fig. 5. To determine the threshold we restricted the linear regression to fluences below 6 J cm^{-2} because these experiments were conducted at atmospheric pressure. By comparing the results to experiments in vacuum and by checking the interferometric autocorrelation of the focused pulses we realized that there is no significant distortion of the 5-fs pulses by plasma formation in air up to this level. On the other hand, the measured volumes above this level only slightly deviate from the regression line. The single-shot experiments had to be carried out in vacuum because of the higher damage threshold fluence.

The data depicted in Fig. 5 reveal that both, the threshold fluence for ablation and the average ablated volume per pulse are significantly different for multi-shot and single-shot excitation. This means that for a certain laser fluence above both thresholds a single pulse ablates much more material than a pulse of a series of 50 pulses does on an average.

These results may be interpreted in terms of a pre-ablation modification of the irradiated material while working with a laser fluence between the two threshold fluences. Here, the first laser pulse encounters the original fused silica and already alters the material. This alteration might be for instance the formation of color centers as summarized in Ref. [21]. All the possibilities of material modification mentioned there result in the generation of electronic states within the forbidden gap, which culminate in an enhanced light absorption of the sample compared to the multiphoton absorption process presumed for

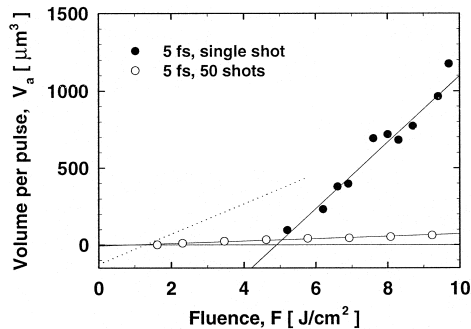


Fig. 5. Volume V_a of fused silica ablated by one laser pulse versus laser fluence F for craters generated by a single laser pulse and by 50 laser pulses on the same sample spot, respectively. The straight lines are obtained from linear regression. The intersection of the regression line with the horizontal axis ($V_a = 0$) yields the threshold fluence F_{th} for optical damage. In the case of 50 pulses per spot only data obtained at $F \leq 6 \text{ J cm}^{-2}$ were considered for regression to avoid the influence of plasma formation in air. The dotted line is the 10-fold enhanced regression line for the multi-shot measurements to allow comparison with the single-shot data.

the unaltered fused silica. This increased absorption finally leads to a lower damage threshold in the case of multiple pulses onto the same spot and a lower penetration depth of the laser radiation and therefore a smaller ablation depth and ablation volume. According to these results, the incubation effects take place in fused silica even at pulse durations as short as 5 fs, which is supported by the observation, that single pulse irradiation of fused silica with a fluence between these two thresholds leads to coloring of the sample.

4. Conclusions

Micromachining of dielectrics with laser pulses in the 10-fs range shows some important features as compared to longer pulses of several 100 fs. For the shortest pulses used, the statistical character of the material removal is strongly reduced, resulting in a significantly improved reproducibility and controllability of the ablation process. The extremely high machining precision achieved with pulses in this time domain will allow the fabrication of submicron-sized microstructures in materials with very high reproducibility.

Investigating incubation phenomena, we compared the damage threshold fluences for obtained for irradiation with single pulses and multiple pulses on the same spot. With 5-fs pulses on fused silica we found the damage threshold to be about four times enhanced for the single-shot case. We also noticed a significant decrease in the ablation rate for pre-irradiated fused silica. These observations lead us to the conclusion that incubation effects alter the optical properties of the material even for pulses as short as 5 fs.

Acknowledgements

We wish to thank Gabriele Pfeiffer and Harald Bergner from the Fachhochschule Jena, Germany for invaluable help with the AFM measurements. M.L.

acknowledges support from the Austrian Science Fund (FWF) under grant number P-12762. W.K. is grateful for partial support by the EU Brite-Euram III project # BRPR-CT96-0265 and by the German BMBF project # 13N-7048/7.

References

- [1] R. Srinivasan, E. Sutcliffe, B. Braren, *Appl. Phys. Lett.* 51 (1987) 1285.
- [2] S. Preuss, M. Späth, Y. Zhang, M. Stuke, *Appl. Phys. Lett.* 62 (1993) 3049.
- [3] J. Krüger, W. Kautek, *Appl. Surf. Sci.* 96–98 (1996) 430.
- [4] B.C. Stuart, M.D. Feit, A.M. Rubenchik, B.W. Shore, M.D. Perry, *Phys. Rev. Lett.* 74 (1995) 2248.
- [5] H. Varel, D. Ashkenasi, A. Rosenfeld, R. Herrmann, F. Noack, E.E.B. Campbell, *Appl. Phys. A* 62 (1996) 293.
- [6] D. von der Linde, H. Schüller, *J. Opt. Soc. Am. B* 13 (1996) 216.
- [7] J. Ihlemann, B. Wolff, P. Simon, *Appl. Phys. A* 54 (1992) 363.
- [8] D. Du, X. Liu, G. Korn, J. Squier, G. Mourou, *Appl. Phys. Lett.* 64 (1994) 3071.
- [9] P.P. Pronko, S.K. Dutta, J. Squier, J.V. Rudd, D. Du, G. Mourou, *Opt. Comm.* 114 (1995) 106.
- [10] D. Ashkenasi, A. Rosenfeld, H. Varel, M. Wähmer, E.E.B. Campbell, *Appl. Surf. Sci.* 120 (1997) 65.
- [11] D. Stern, R.W. Schoenlein, C.A. Puliafito, E.T. Dobi, R. Birngruber, J.G. Fujimoto, *Arch. Ophthalmol.* 107 (1989) 587.
- [12] W. Kautek, J. Krüger, *Proc. SPIE* 2207 (1994) 600.
- [13] F.H. Loesel, M.H. Niemz, J.F. Bille, T. Juhasz, *J. Quant. Electron.* 32 (1996) 1717.
- [14] S. Sartania, Z. Cheng, M. Lenzner, G. Tempea, Ch. Spielmann, F. Krausz, *Opt. Lett.* 22 (1997) 1562.
- [15] M. Nisoli, S. Stagira, S. De Silvestri, O. Svelto, S. Sartania, Z. Cheng, M. Lenzner, Ch. Spielmann, F. Krausz, *Appl. Phys. B* 65 (1997) 189.
- [16] J. Krüger, W. Kautek, *Appl. Surf. Sci.* 96–98 (1996) 430.
- [17] D. von der Linde, H. Schüller, *J. Opt. Soc. Am. B* 13 (1996) 216.
- [18] J.M. Liu, *Opt. Lett.* 7 (1977) 196.
- [19] M. Lenzner, J. Krüger, S. Sartania, Z. Cheng, Ch. Spielmann, G. Mourou, W. Kautek, F. Krausz, *Phys. Rev. Lett.* 80 (1998) 4076.
- [20] N. Bloembergen, *IEEE J. Quant. Electron.* QE-10 (1974) 375.
- [21] D. Bäuerle, in: *Laser Processing and Chemistry*, Springer, Berlin, 1996, p. 225.